FULL LENGTH	Iranian Biomedical Journal 29 (5): 294-308 September 2025

Chloroquine Enhances *Mda-7*- Induced Apoptosis via *miR-7* and HSP70 Modulation in Glioblastoma

Seyedeh Maliheh Babazadeh[1], Mohammad Reza Zolfaghari[1*], Mohsen Zargar[1], Kazem Baesi[2], Amir Ghaemi[3*]

[1]Department of Microbiology, Qo.C., Islamic Azad University, Qom, Iran; [2]Hepatitis and AIDS Department, Pasteur Institute of Iran, Tehran, Iran; [3]Department of Influenza and other Respiratory Viruses, Pasteur Institute of Iran, Tehran, Iran

OPEN ACCESS

Article type: Research Article
Received: July 21, 2025
Revised: August 16, 2025
Accepted: August 30, 2025
Published online: August 31, 2025

How to cite:
Babazadeh SM, Zolfaghari MR, Zargar M, Baesi K, Ghaemi A. Chloroquine Enhances *Mda-7*- Induced Apoptosis via *miR-7* and HSP70 Modulation in Glioblastoma. *Iran. Biomed. J.* 2025; 29(5): 294-308.

ABSTRACT

Background: *Melanoma differentiation-associated gene-7* (*Mda-7)* selectively suppresses growth and induces apoptosis in various tumor cells without harming normal cells. Inhibition of autophagy has been shown to enhance the efficacy of many cancer therapies. However, its effect on the anticancer activity of Ad/*Mda-7* in GBM has remained unclear. This study investigated the combined effect of an autophagy inhibitor (CQ) and *Mda-7* in U87 cancer cells.

Methods: Cell proliferation was assessed using the MTT assay. Apoptosis rates, autophagy induction, and ROS levels were measured using flow cytometry. Caspase-9 and β-actin protein levels were analyzed by Western blotting. ELISA was employed to quantify HSP70 and TRAIL level in the culture medium. Real-time PCR evaluated the expression levels of cell death-related genes (*P38 MAPK*, *Bax*, and *TRAIL*) and specific miRNAs (*miR-7*, *miR-122*, and *miR-21*) in treated cells.

Results: Combined treatment with Ad/*Mda-7* and the autophagy inhibitor CQ significantly reduced cell viability and proliferation. Ad/*Mda-7* induced LC3-II protein expression in U87 cancer cells, which was further increased by autophagy inhibition through CQ. The combination treatment also increased apoptosis rates, elevated ROS levels, and decreased HSP70 protein expression, highlighting its synergistic anticancer effects. Increasing the expression of *miR-7* and *miR-122* indicated that the elevated levels of these endogenous miRNAs may help improve the treatment process.

Conclusion: Our findings indicate that the combination of Ad/*Mda-7* and CQ synergistically could inhibit U87 cancer cell growth and could serve as a promising approach for treating human GBM. ***DOI: 10.61882/ibj.5131***

Keywords: Ad/*Mda-7*, Chloroquine, Apoptosis, Autophagy, Glioblastoma

Corresponding Authors:
Mohammad Reza Zolfaghari
Department of Microbiology, Qo.C., Islamic Azad University, Qom, Iran. P.O.Box: 3749113191; Tel.: (+98-912) 4513783; Fax: (+98-253) 2805797; E-mail: mreza.zolfaghary@gmail.com , mo.zolfaghari123@iau.ir; ORCID ID: 0000-0002-4265-0543

Amir Ghaemi
Influenza and Respiratory Viruses Department, Pasteur Institute of Iran, Tehran, Iran P.O. Box: 1316943551; Tel.: (+98-21) 64112187; Fax: (+98-21) 2164112187; E-mail: ghaem_amir@yahoo.com; a_ghaemi@pasteur.ac.ir; ORCID ID: 0000-0001-7793-2920

List of Abbreviations:
Ad/*Mda-7*: adenoviruses expressing *melanoma differentiation-associated gene-7*; **BafA1:** bafilomycin A1; **BSA:** bovine serum albumin; **CQ:** chloroquine; **DCFH-DA:** dichlorofluorescein diacetate; **DMEM:** dulbecco's minimal medium; **DMSO:** dimethyl sulfoxide **ECL:** electrochemiluminescence; **ELISA:** enzyme-linked immunosorbent assay; **ERK:** extracellular signal-regulated kinase; **GBM:** glioblastoma; **HRP**: horse reddish peroxidase; **HSP70:** heat shock protein of 70; **LC3-II:** light chain 3-II protein; ***Mda-7*:** melanoma differentiation-associated gene 7; **microRNA:** miRNA; **MOI:** multiplicity of infection; **PE:** phycoerythrin; **PI**: propidium Iodide; **ROS:** reactive oxygen species; **RTK:** receptor tyrosine kinases; **SDS-PAGE:** sodium dodecyl sulfate-polyacrylamide gel electrophoresis; **TRAIL:** tumor necrosis factor-related apoptosis-inducing ligand

[DOI: 10.61882/ibj.5131]

INTRODUCTION

Glioblastoma, often known as grade IV astrocytoma, is the most invasive type of tumor originating from glial cells. It is the most common and nearly mortal neoplasm of the central nervous system and shows a high resistance to standard treatments such as surgery, chemotherapy, and radiation therapy. Recently, gene therapy has gained increasing attention as a potential approach for cancer treatment. In this method, a therapeutic gene is delivered to target cells.

Mda-7, also known as *IL-24*, is a unique member of the IL-10 family of cytokines with ubiquitous tumor-suppressive properties. Its antitumor activities include the inhibition of angiogenesis, invasion, and metastasis, as well as the enhancement of cancer cell sensitivity to chemotherapy and induction of cancer-specific apoptosis[1]. Given its widespread apoptotic action on cancerous cells and minimal effects on healthy cells, along with few side effects, *Mda-7* is considered an important candidate for cancer therapy[2,3]. However, despite extensive studies, questions remain about how to further enhance the antitumor effects of *Mda-7*.

Autophagy has received special attention as a mechanism through which cancer cells develop resistance to therapy[4]. Autophagy manipulation has also been proposed as a valuable strategy to prevent tumor development and limit its progression. Although GBM cells are typically resistant to the apoptosis-inducing therapies, they may exhibit heightened sensitivity to treatments targeting autophagy[5]. Autophagy often prevents the initiation of apoptosis, while the activation of apoptosis-related caspases can inhibit the autophagic processes[6,7]. Therefore, autophagy inhibitors are considered effective tools to increase the effectiveness of anticancer treatments[8]. The cancer-specific chemosensitizing effect of chloroquine (CQ) depends, in part, on its ability to inhibit autophagy[9,10]. CQ can inhibit autophagy by preventing lysosomal acidification and autophagosomes-lysosome fusion, thereby blocking autolysosome degradation at the final stage of autophagy[11,12].

Studies have shown that CQ has antitumor activity in various cancer types, including GBM[13,14], hepatocellular carcinoma[15], breast cancer[16], prostate cancer[17], and pancreatic cancer[18]. In our previous study, we showed that *Mda-7* induces cancer-specific apoptosis through mechanisms involving both apoptosis or autophagy toxicity[19]. However, it has not been investigated whether autophagy inhibition could enhance the anticancer effect of *Mda-7* in GBM. Moreover, recent studies have highlighted the role of miRNAs in regulating autophagy and the importance of autophagy progression in different stages of cancer and its treatment[20,21].

This study aimed to explore the relationship between autophagy inhibition and increased apoptosis induced by the *Mda-7* gene in a human GBM cell line. Specifically, it focused on elucidating the signaling pathways involved in cell death, assessing its impact on the expression of relevant miRNAs and identifying potential diagnostic and therapeutic biomarkers.

MATERIALS AND METHODS

Cell culture and in vitro infection of cells with Ad/*Mda-7*

The human GBM cell line U87 is commonly used in brain tumor research. The human embryonic kidney cell line 293 (HEK-293) performs dual functions for adenovirus production and amplification. Recombinant serotype 5 Ad/*Mda-7* was produced in HEK-293 cells. Both cell lines were purchased from the National Cell Bank of the Pasteur Institute of Iran (Tehran). The cells were cultured in high-glucose DMEM comprising 10% fetal bovine serum (Gibco, Grand Island, NY, USA), 15 mM of HEPES, penicillin (100 U/ml), and streptomycin (100 µg/ml) in an environment containing 5% CO_2 at 37 °C.

Measurement of cell viability and synergistic effect analysis

Cell viability was assessed using the MTT method. U87 cells were seeded into 96-well microplates (3.0×10^4 cells/well). After incubating in the presence of 5% CO_2 and humidity at 37 °C for 24 h, the cells were infected with Ad/*Mda-7* at different MOIs: 1, 3, 5, 7, and 10, for 2 h. Subsequently, the cells were treated with different concentrations of CQ (20, 40, 60, 80, and 100 µM). Following a 48 h incubation, 100 µl of MTT solution was added to each well and incubated at 37 °C for 3 h. The incubation medium was then removed, and 100 µl of DMSO was added to dissolve formazan crystals. Cells without any treatment were used as controls. Absorbance was measured at 540 nm using a microplate reader (Anthos Labtech Instruments, Austria) to assess MTT reduction. Each test was measured three times (n = 3). According to the MTT results and to ensure the validity of the effective concentration, the synergistic effect and combination score were calculated using Combenefit software (v2.021; developed by the Cancer Research UK Cambridge Institute). The software was used for isobologram analysis and correlation determination. The HSA model was selected to assess dose-response relationships and synergism distribution of a single agent.

[DOI: 10.61882/ibj.5131]

Experimental design

Based on the results of the synergism analysis, the antitumor efficacy of the combined treatment using the optimal MOI of Ad/*Mda-7* and the optimal concentration of CQ was evaluated. Cell viability was experimentally investigated in both monotherapy and combined treatment groups using the MTT method. Then, various factors involved in apoptosis- and autophagy-related signaling pathways, such as Annexin/PI, caspase-9, p38 MAPK, TRAIL, Bax, LC3-II, ROS, HSP70, and miRNAs (miR-7, miR-21, and miR-122), were investigated.

Measurement of activated autophagy

To perform this procedure, we seeded 3×10^5 U87 cells into each well of a 24-well plate. According to the synergism analysis, the cells were treated with the optimal MOI of Ad/*Mda-7* and effective concentration of CQ, either as monotherapy or in combination. Autophagy induction associated with autophagosome formation was assessed using specific antibodies and flow cytometry. Cells were suspended 48 h after infection and fixed in 4% formaldehyde for 15 minutes. To enhance permeability, the cells were treated with 0.2% Triton X-100 for 10 minutes at room temperature. Then, the cells were labeled for 30 minutes with a primary antibody against LC3-II (Abcam, USA) diluted in PBS containing 1% BSA. After washing with PBS, a PE-conjugated secondary antibody (donkey anti-IgG, BioLegend, USA) was added and incubated at room temperature for 30 min. Cells were analyzed by flow cytometry (Becton & Dickinson Biosciences, USA). Each test was measured twice (n = 2).

Apoptosis analyses by flow cytometry

Cellular apoptosis was analyzed using the PE annexin-V/PI apoptosis detection kit (BioLegend, USA). After culturing the cells in a 24-well plate and infecting them with Ad/*Mda-7* with or without CQ, the amount of cell apoptosis was investigated after 48 h. The cells were detached using a scraper, collected from the wells by adding 2 ml of PBS solution, then centrifuged and washed. After removing the culture medium, the cell pellet was resuspended in 1× binding buffer. The anti-annexin V/PI staining antibody conjugated with polyethylene was used (BioLegend, USA). To compensate for color overlap between PE and PI, we employed 7-AAD dye. After the incubation period, 1× buffer solution was added to the tubes. Following centrifugation, 1× binding buffer was added to the cell pellet. Finally, the samples were analyzed using a BD FACS Calibur machine (BD Biosciences, San Jose, CA, USA), with PE-V annexin detected at a wavelength of 578 nm in the H-FL2 channel and PI dye at 647 nm in the H-FL3 channel.

Measurement of intracellular ROS

The amount of intracellular reactive oxygen species (ROS) was measured using 2,7- dichlorofluorescein diacetate (DCFH-DA) (Sigma-Aldrich, USA). Briefly, U87 cells were seeded at a density of 3×10^5 cells per well in 24-well plates. The amount of ROS produced in the cells treated with Ad/*Mda-7*, with or without CQ, was examined after 48 h of incubation. After incubating with DCFH-DA for one hour, the samples were trypsinized and rinsed with phosphate-buffered saline (PBS). Eventually, the severity of cell fluorescence was determined by the flow cytometry (BD Biosciences, USA). Each test was carried out twice (n = 2).

Western blot analysis

Apoptosis induced by Ad/*Mda-7* and CQ, administered as monotherapy or in combination, was evaluated using the Western blotting method, focusing on caspase-9 as a key apoptotic marker. After 48 h of treatment, cultured cells were lysed using radioimmunoassay buffer (RIPA, Beyotime Biotechnology, China). Proteins were then separated by 12% SDS-PAGE and transferred to a polyvinylidene difluoride membrane (Sigma, USA). After blocking the membrane with BSA, it was exposed to primary antibodies for anti-caspase 9 and anti-actin (as a loading control) at a dilution of 1:1000 (Abcam) at 4°C overnight. Next, the cells were washed and incubated with a rabbit anti-mouse antibody (1:10,000; Sigma). Finally, protein bands were visualized by chemiluminescence using an ECL detection system (Amersham Pharmacia Biotech, Buckinghamshire, UK). Densitometric analysis of the proteins was performed using J software (NIH, Bethesda, USA).

Real-time RT-PCR

A high-performance isolation kit (Roche, Germany) was used to extract total RNA from the U87 cell line according to the manufacturer's instructions. The amount of RNA was determined by a nanodrop spectrophotometer. For the analysis of miRNA, complementary DNA synthesis was initiated from 1 µg of total RNA using the BON Stem High Sensitivity miRNA Kit (BON001027SL, Iran) following the manufacturer's instructions. The reaction mixture included the BON-RT adapter, reverse transcriptase, RT buffer containing Mg^{2+}, dNTPs, oligo-dT primers, and random primers. Reverse transcription was performed using a thermocycler (Applied Biosystems, USA) with a program as follows: 25 °C for 10 min, 42 °C for 60 min, and 72 °C for 10 min. Real-time PCR analysis was performed using the SYBR Green method on a Bio-Rad, USA machine. For each PCR reaction, a master mix—containing 2 µl of DNA, 4 µl of Hot Firepole Eva Green

[DOI: 10.61882/ibj.5131]

qPCR Mix (Solis BioDyne, Estonia), and 0.2 mM of each reverse and forward primer—was prepared on ice. The final volume was adjusted to 20 µL with H_2O. Primer sequences for target genes *(P38*, *MAPK*, *TRAIL*, and *Bax*) and the housekeeping gene *β-actin* were designed using Primer-BLAST software (NCBI). MiRNAs (*miR-7*, *miR-21*, and *miR-122*) and their predicted targets were measured in cells and tissues using real-time reverse transcription PCR with the SYBR Green dye on a Bio-Rad CFX96 system. MiRNA expression levels were determined relative to the target sequence (Ct) and normalized to the *U6* expression level. The $2^{-\Delta\Delta CT}$ method was then used to compare mRNA levels between treatment and control groups to determine statistical difference for data analysis. Each experiment was repeated twice. The miRNA primers were synthesized by the Stem Cell Technology Research Center and produced along with other primers by Sinaclone, IRAN Trading Company (Table S1).

Enzyme-linked immunosorbent assay

Human HSP70 and TRAIL ELISA kits (Abcam) were used to measure the levels of HSP70 and TRAIL in viral lysate. The U87 cells were infected with Ad/*Mda-7* at a MOI of 5 and treated with 60 µM of CQ. After 48 h, the cell supernatant was collected. The cell lysates were filtered using 40 µm filters and centrifuged at 3300 ×g at 4 °C for 10 minutes. The concentration of viral protein in the lysate was then adjusted to 2 mg/ml with PBS. Monoclonal antibodies were coated onto 96-well plates, and samples were added to the wells. An HRP-conjugated anti-IgG antibody was subsequently applied and incubated. After washing the plate, a TMB substrate was added, which reacts with HRP to produce a blue color. After adding a stop solution, the color changed to yellow, and absorbance was measured at 450 nm. Each experiment was repeated three times and analyzed (n = 3).

Statistical analysis

Statistical analysis was performed using GraphPad Prism (GraphPad Prism 8.4.3, CA, USA). Group differences were evaluated using one-way ANOVA, followed by Tukey's post hoc analysis. *P* values less than 0.5 were considered statistically significant.

RESULTS

Synergistic effect of Ad/*Mda-7* and CQ

The synergistic effect of combining Ad/*Mda-7* with CQ was evaluated using Combenefit software. U87 cell viability was assessed after treating the cells with different MOIs (1, 3, 5, 7, and 10) of Ad/*Mda-7* and varying concentrations of CQ (20, 40, 60, 80, and 100 µM) as monotherapies (Fig. 1A and 1B). The analysis of the monotherapy experiments using Combenefit software revealed that an MOI of 5 for Ad/*Mda-7*, when combined with CQ concentrations higher than 20 µM, exhibited the strongest synergistic effect (Fig. 1C). To further validate these findings, we examined combination therapy using Ad/*Mda-7* at an MOI of 5, along with various concentrations of CQ. As shown in Fig. 1D, the combination of Ad/*Mda-7* (MOI 5) with 60 µM of CQ, significantly inhibited the growth and proliferation of U87 cells compared to control cells ($p < 0.0001$).

Synergetic effect of Ad/ *Mda-7* and CQ on GBM

Ad/*Mda-7* and CQ exhibited a synergistic effect on GBM. The impact of Ad/*Mda-7* or CQ on cell viability in U87 cell lines was assessed after 48 h of treatment. Antitumor effects was evaluated using monotherapy with Ad/*Mda-7* at a MOI of 5 and CQ at 60 µM. The synergistic effect of combination therapy was further compared to control cells using the MTT reduction method. As depicted in Figure 2, the percentage of viable cells after treatment was 75.44% for Ad/*Mda-7* alone, 81.52% for CQ alone, and 54.28% for the combination therapy. Therefore, the synergistic effect of the combination therapy on U87 cells was significantly evident when compared to both the monotherapy groups ($p < 0.0001$) and the control group ($p< 0.001$).

CQ inhibited autophagy induced by Ad/*Mda-7*

LC3-II expression serves as a pivotal marker for assessing the autophagy progression. Utilizing flow cytometry analysis, we monitored the conversion of human LC3 protein from its cytoplasmic state (LC3-I) to the autophagosomal form (LC3-II) in U87MG cells. CQ, a late-phase autophagy inhibitor, prevents the autophagosome degradation, leading to LC3-II accumulation. Our investigation focused on analyzing the expression levels of LC3-II protein in monotherapy—Ad/*Mda-7* alone and CQ alone—as well as in combination therapy, compared to the control cells. Figure 3 illustrates that the levels of LC3-II protein in the monotherapy groups with Ad/*Mda-7* (93.5%) and CQ (85.75%) was significantly higher than the level of this protein in the control group (76.65%). Additionally, the combination therapy group (98.9%) exhibited a significant increase in LC3-II protein accumulation compared to monotherapy with Ad/*Mda-7* ($p < 0.005$) or CQ ($p < 0.002$), as well as the control group ($p < 0.0001$). This increasing trend remained consistent over the period of 48 h, demonstrating sustained elevation in LC3-II levels.

[DOI: 10.61882/ibj.5131]

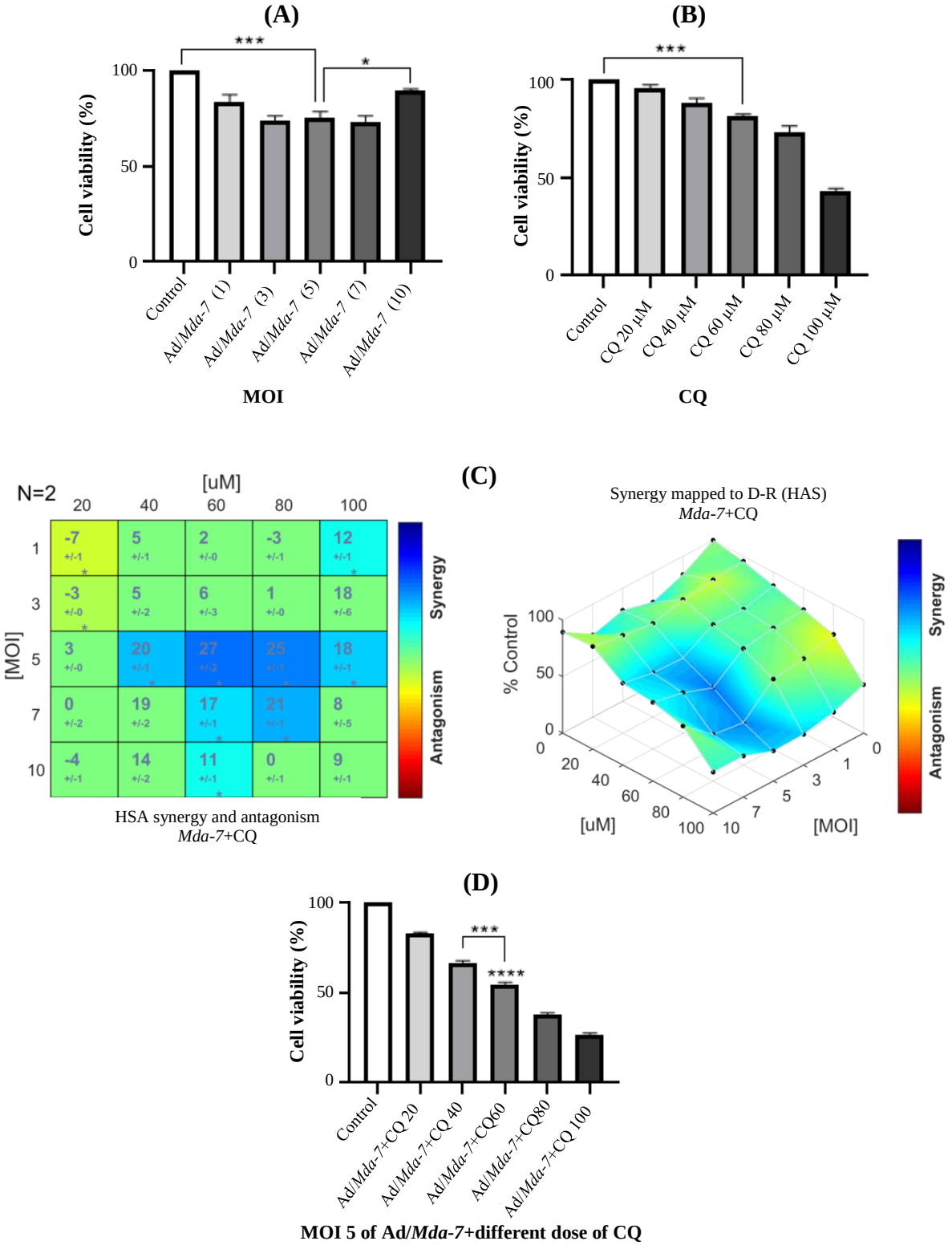

Fig. 1. Evaluation of U87 cell viability following treating the cells with different MOIs of Ad/Mda-7 and varied concentrations of CQ . (A) Treatment of U87 cells with different MOIs of Ad/*Mda-7*; (B) The effect of different concentrations of CQ on viability of U87 cells; (C) Isobologram analysis and determination of synergism in combination therapy for U87 cells using Combenefit software. Data represent three independent experiments (n = 3); (D) Confirmation of the appropriate concentration of CQ combined with the optimal MOI of Ad/*Mda-7*, as determined by Combenefit isobologram analysis, using the MTT method. One-way ANOVA analysis revealed a statistically significant decrease in cell survival resulting from the combination treatment of the optimal MOI of Ad/*Mda-7* with the appropriate concentration (60 µM) of CQ. ($^{****}p < 0.0001$).

[DOI: 10.61882/ibj.5131]

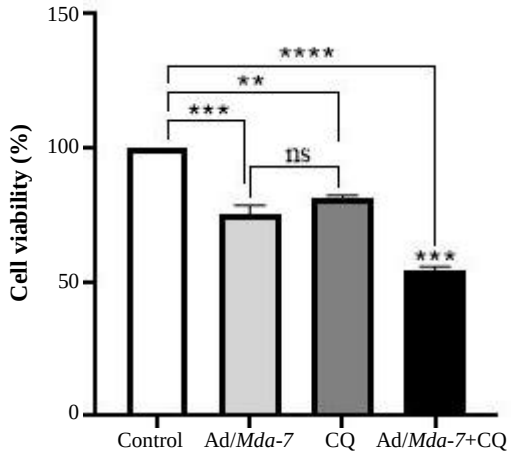

Fig. 2. Viability assessment of U87 cells treated with Ad/*Mda-7* and CQ using MTT assay. U87 cells were treated with an MOI 5 of Ad/*Mda-7* and 60 μM of CQ, alone or in combination, and cell survival was measured after 48 h. Untreated cells were used as the control. One-way ANOVA analysis showed statistically significant reduction in cell viability in the combination treatment group compared to the control group ($^{**}p < 0.001$; $^{***}p < 0.0004$; $^{****}p < 0.0001$) ns: not significant.

Inhibition of autophagy enhanced Ad/*Mda-7*-mediated apoptosis

To investigate whether combination therapy can enhance antitumor effects and also induce cell apoptosis in GBM cells, we assessed the amount of apoptosis in U87 cells in monotherapy groups Ad/*Mda-7* or CQ groups alone, or in combination therapy at 48 h after infection using annexin V/PI double staining. As shown in Figure 4, the rates of cell apoptosis in the monotherapy groups with Ad/*Mda-7* (6.68%) and CQ (31.4%) were significantly higher than that of control group (0.7%). Notably, the combination therapy group showed an apoptosis rate of 39%, which was significantly greater than that observed in the Ad/*Mda-7* alone and the control group ($p < 0.0001$), as well as the CQ monotherapy ($p < 0.005$).

Co-treatment with Ad/*Mda-7* and CQ increased ROS production

The production of ROS is a basic mechanism for antitumor action, which causes apoptosis in cancer cells[22]. Using flow cytometry with DCFH-DA, we determined the ROS levels of the cells to assess whether cell death is associated with increased ROS levels in U87 cell lines. As shown in Figure 5, the ROS production in the Ad/*Mda-7* (76.4%) and CQ (86.9%) monotherapy groups was significantly higher than that of the control group (44.6%). Moreover, the combination therapy (98.5%) resulted in a statistically significant increase in ROS level compared to both the Ad/*Mda-7* monotherapy ($p < 0.001$) and control ($p < 0.0006$) groups. However, there was no significant difference in ROS level when compared to the CQ monotherapy group.

Co-treatment with Ad/*Mda-7* and CQ affected gene expression levels in U87 cells

After treating U87 cell lines with Ad/Mda-7 or CQ groups alone or in the combination treatment group, the expression levels of the genes involved in the cell death pathway were analyzed using real-time PCR. Also, endogenous miRNA expression levels were assessed after treatment of U87 cell line compared to the control group. Figure 6A-6C illustrates the expression levels of the *miR-7*, *miR-21*, and *miR-122* genes after treatment with Ad/*Mda*-7 and CQ as monotherapy or combination therapy. The results showed a significant difference between the *miR-7* expression in the combined treatment group and CQ monotherapy ($p < 0.005$) compared to the control group ($p < 0.004$). However, Ad/*Mda-7* monotherapy did not significantly elevate *miR-7* expression relative to the control group. *miR-21* gene expression significantly increased in the Ad/*Mda-7* monotherapy group ($p < 0.01$) compared to the control group, while no significant differences were observed between the control group and the other treated groups. *miR-122* gene expression significantly increased in all treated groups, including combined treatment ($p < 0.0009$), monotherapy with CQ ($p < 0.001$), and Ad/*Mda-7* ($p < 0.0001$), compared to the control group. As shown in Figure 6D-6F, the expression levels of the *P38 MAPK*, *TRAIL*, *Bax*, and genes were significantly increased in the combination treatment group, as well as in the Ad/*Mda-7* or CQ monotherapy groups ($p < 0.0009$).

Co-treatment with Ad/*Mda-7* and CQ enhanced caspase-9 expression in U87 cells

The expression levels of caspase-9 were evaluated in the groups treated with Ad/*Mda-7*, CQ, or their combination, after 48 h using Western blotting method (Fig. 7). The expression levels of caspase-9 were quantified using Image J software and normalized to β-actin density. The results showed a significant increase in the caspase-9 protein level in the combination treatment group compared to the CQ monotherapy group ($p < 0.003$) and the control group, as well as the Ad/*Mda-7* monotherapy ($p < 0.01$).

Co-treatment with Ad/*Mda-7* and CQ affected the protein levels of HSP70 and TRAIL

HSP70 is considered as an anti-apoptotic factor that enables cells to avoid programmed cell death, whereas TRAIL serves as a key initiator of cell death signaling

[DOI: 10.61882/ibj.5131]

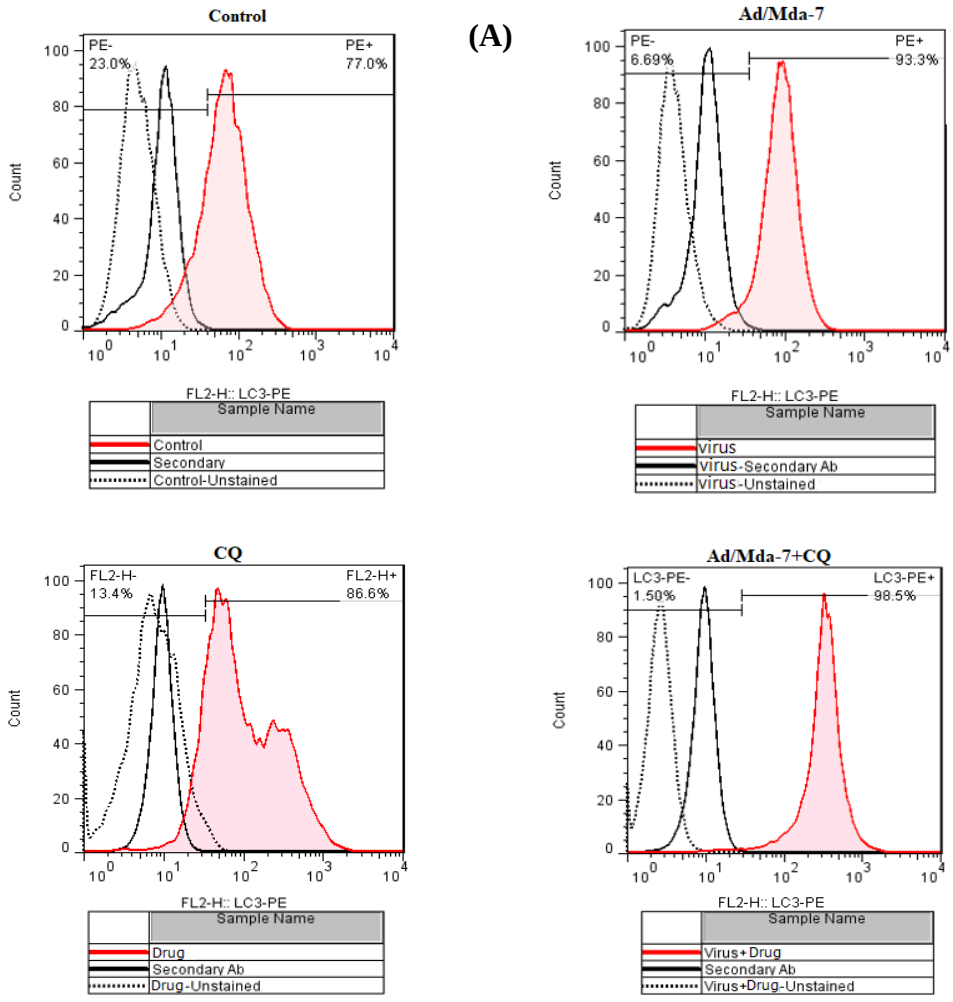

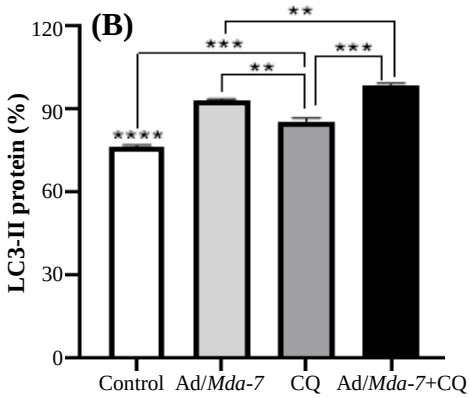

Fig. 3. LC3-II labeling of the U87 cell line after treatment with Ad/*Mda-7* and CQ. (A) U87 cells were inoculated with Ad/*Mda-7* and CQ groups as monotherapy or combination therapy for 48 h, stained with secondary antibodies, and analyzed using flow cytometry. Untreated cells were used as a control; (B) Comparison of LC3-II protein accumulation in different treated group, showing that the combination treatment could significantly increase the LC3-II level compared to the other groups. One-way ANOVA analysis indicated a statistically significant difference between the combination treatment and monotherapy with Ad/*Mda-7* ($^{**}p < 0.005$) or CQ ($^{***}p < 0.002$), and the control group ($^{****}p < 0.0001$).

[DOI: 10.61882/ibj.5131]

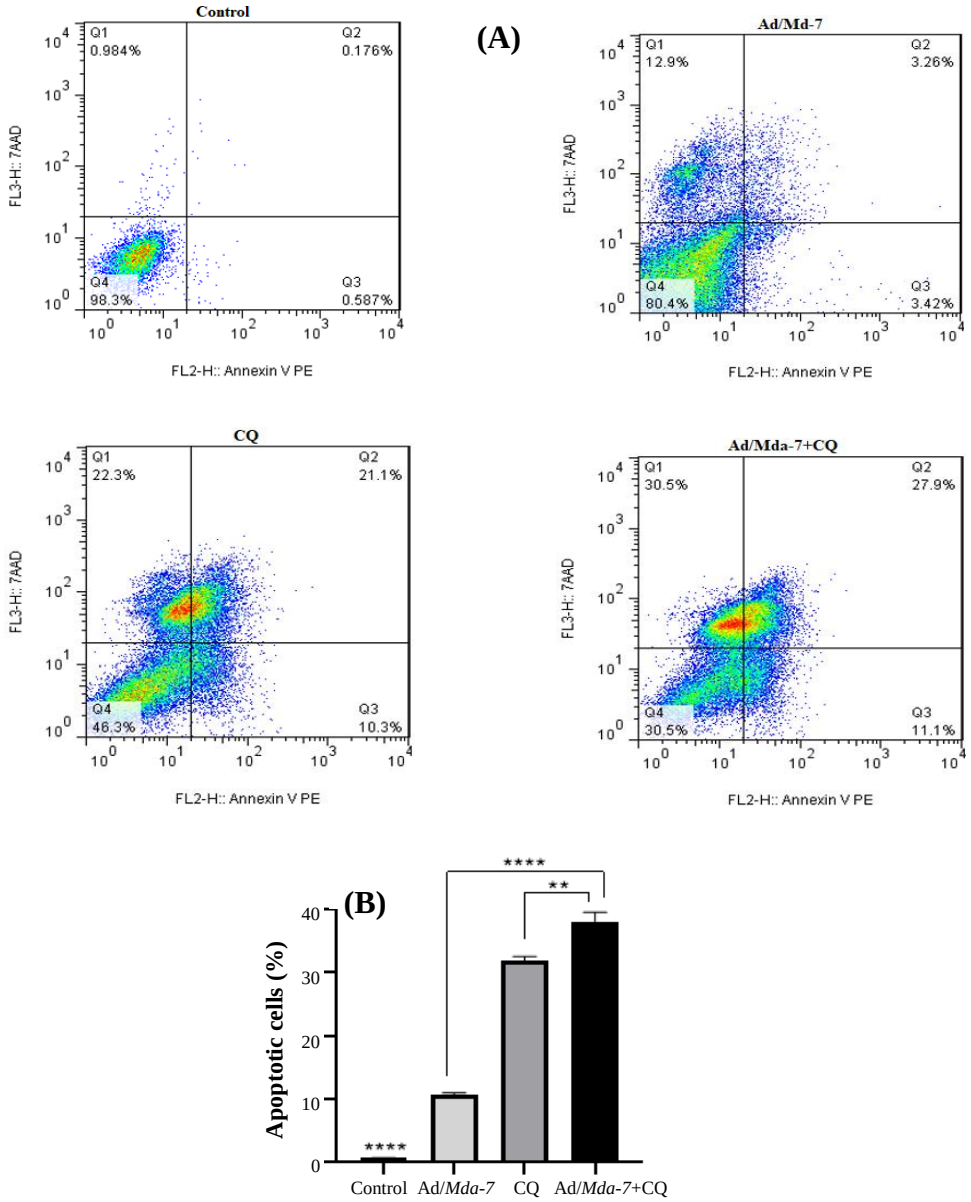

Fig. 4. Annexin V/PI staining of the U87 cells. (A) U87 cells were infected with Ad/*Mda-7* and CQ as monotherapy or combination treatment for 48 h, labeled with annexin V/PI and evaluated using flow cytometry method. Uninfected cells were used as a control; (B) A statistically significant difference was found between the combination therapy and other groups. ANOVA analysis (one-way) showed a statistically significant difference between the combination treatment and monotherapy with Ad/*Mda-7* and the control group ($^{****}p < 0.0001$) and to the monotherapy with CQ ($^{**}p < 0.005$).

pathway. We evaluated the protein levels of HSP70 and TRAIL in U87 cell lines treated with Ad/*Mda-7* and autophagy inhibitors using the ELISA method and then compared them to untreated cells. As shown in Figure 8A, HSP70 protein levels were significantly decreased in all treatment groups compared to the control group ($p < 0.0001$). Notably, the combination treatment group exhibited a higher reduction in HSP70 level than those receiving monotherapy with either Ad/*Mda-7* ($p < 0.006$) or CQ ($p < 0.0001$). In Figure 8B, TRAIL protein levels were significantly elevated in both the Ad/*Mda-7* ($p < 0.0001$) and CQ ($p < 0.04$) monotherapy groups when compared to the control group. This increase in protein level was more pronounced in the combination treatment group compared to the monotherapy and control groups ($p < 0.0001$).

[DOI: 10.61882/ibj.5131]

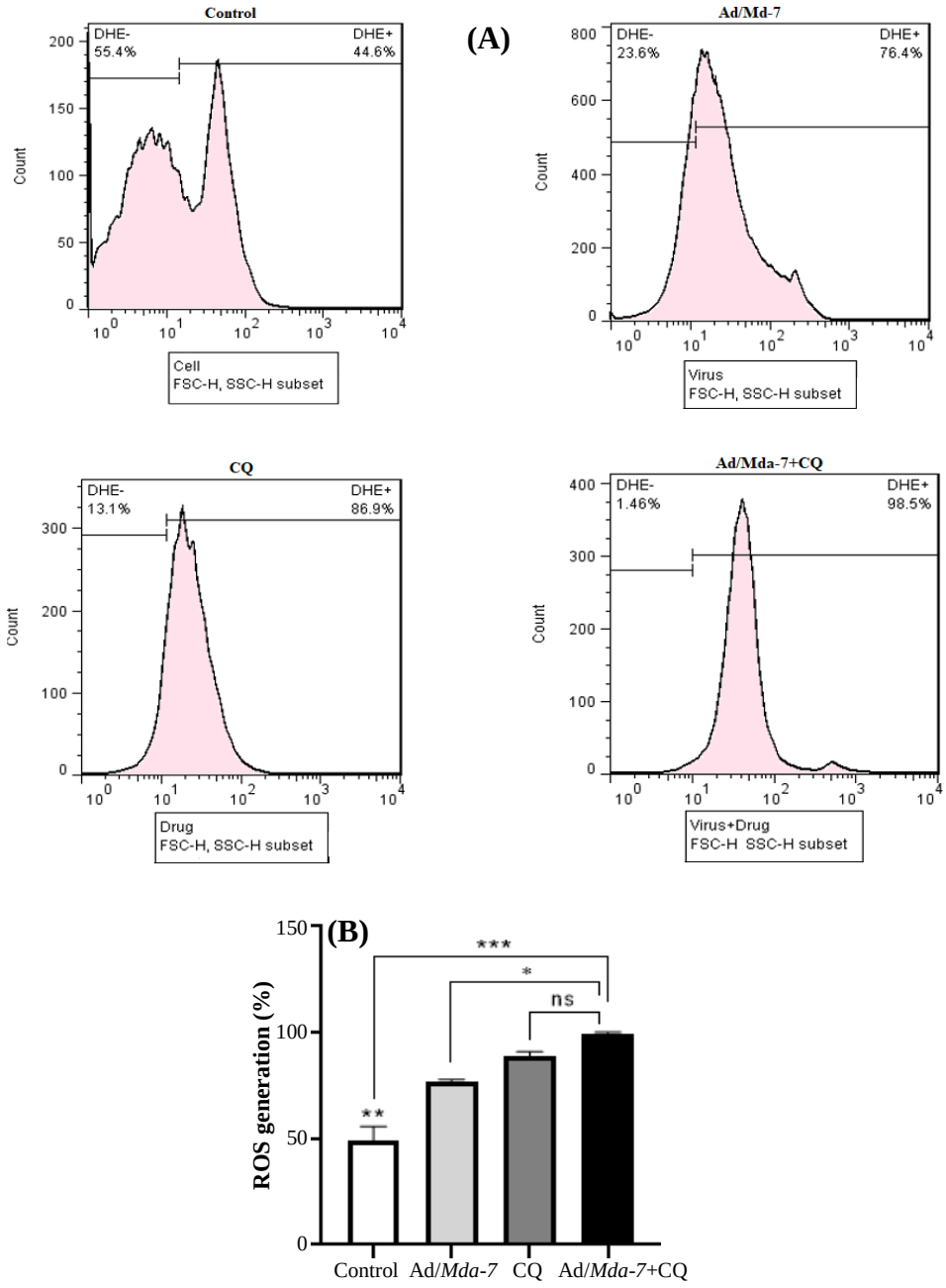

Fig. 5. labeling U87 cell lines with DCFH-DA after treatment with Ad/*Mda-7* and CQ. (A) Flow cytometry was used to evaluate the U87 cells infected with Ad/*Mda-7* and CQ as monotherapy or combination treatment groups after 48 h. The cells were labeled with DCFH-DA, and untreated cells used as control; (B) The combination therapy group produced increased levels of ROS compared to the monotherapy group and the untreated control group. ANOVA analysis (one-way) showed a statistically significant difference between the combination therapy and monotherapy ($^{***}p < 0.0006$) with Ad/*Mda-7* ($^{*}p < 0.001$) and the control group. However, there was no statistically significant difference compared to the CQ monotherapy group.

DISCUSSION

Due to the limitations of traditional glioma treatments, many new therapies, such as antitumor gene therapy, are now widely used in the clinical settings. Generally, cells use autophagy to recycle biomolecules, remove damaged tissues and harmful proteins, and eliminate pathogens in the absence of nutrients. The autophagy pathway plays an important role in maintaining cellular homeostasis and contributes to cell survival under stress. Although apoptosis and autophagy are distinct cellular processes that often have opposing effects, their

[DOI: 10.61882/ibj.5131]

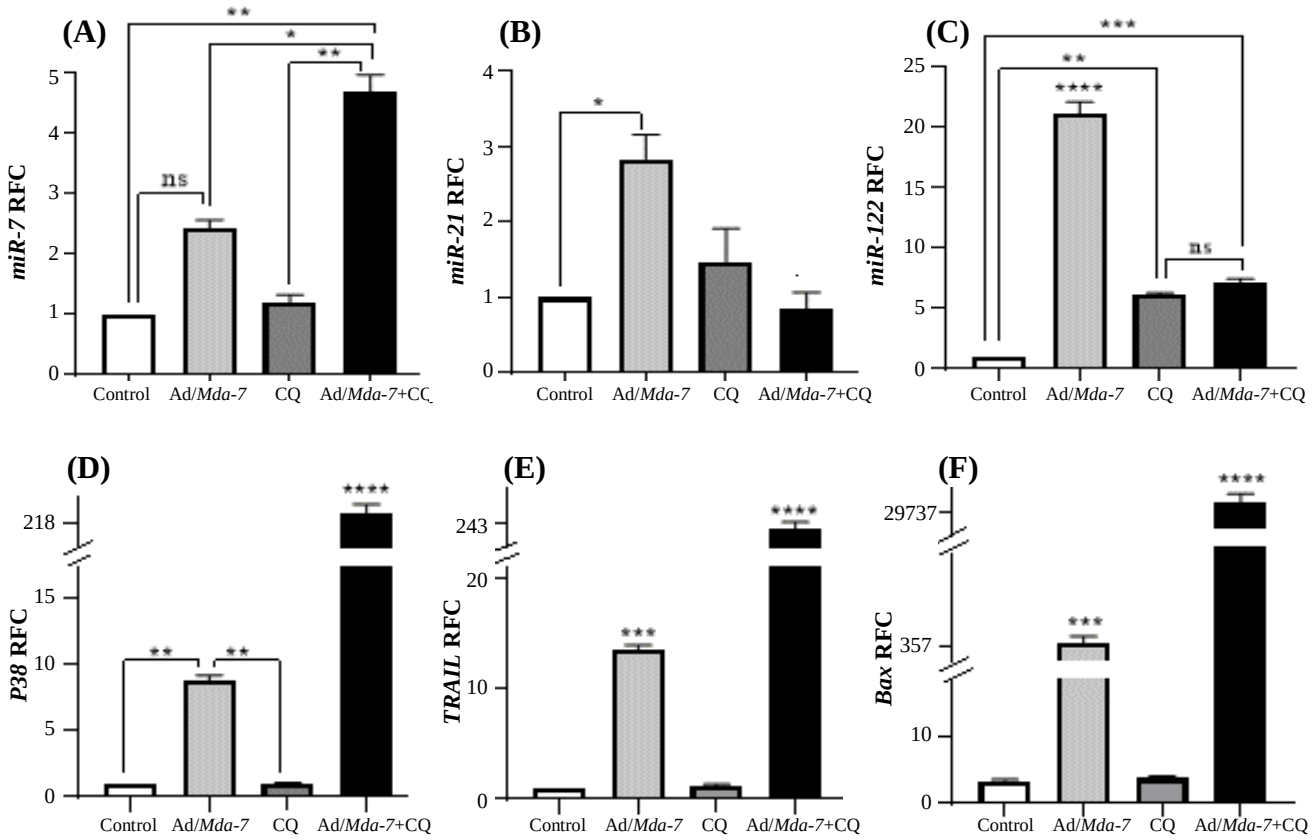

Fig. 6. Analysis of gene expression levels involved in the antitumor pathway in U87 cells treated with Ad/*Mda-7* and CQ. The levels of gene expression were examined 48 h post-treatment using real-time PCR. Uninfected cells served as the control group. (A-C) Comparison of *miR-7*, *miR-21*, and *miR-122* expression levels after monotherapy or combination therapy with Ad/*Mda-7* and CQ; (D-F) Comparison of the expression levels of *P38 MAPK*, *TRAIL*, and *Bax* genes after treatment in the groups treated with Ad/*Mda-7* and CQ. Group differences were evaluated using one-way ANOVA ($^{*}p < 0.01$; $^{**}p < 0.001$; $^{***}p < 0.0009$; $^{****}p < 0.0001$).

signaling pathways are interconnected through different cross-linking mechanisms. Just like cancer, autophagy is also an important factor in the cell death process.

Research has shown that the inhibition of autophagy can increase the effectiveness of antitumor therapies[23]. However, the role of autophagy in cancer is controversial, as it can act as a suppressor or a stimulator depending on the type and stage of tumor[24]. Reports have indicated that inhibiting autophagy in tumor cells can enhance the effects of chemotherapy and increase drug-induced cytotoxicity[25,26]. To investigate whether autophagy inhibition could enhance the apoptosis-induction effect of Ad/*Mda-7*, the well-known autophagy inhibitor, CQ, was administered.

In vitro studies have utilized various lysosomal inhibitors, such as BafA1 and protease inhibitors, along with CQ, to inhibit autophagy. These inhibitors are believed to prevent lysosomal degradation. Among them, only CQ and hydroxychloroquine are FDA-approved drugs that are currently used in clinical trials for treating tumors by inhibiting autophagy[27]. Effective antitumor gene therapy requires a gene that exhibits selective toxicity to target tumor cells without damaging cells or surrounding tissues[28]. As a new member of the IL-10 cytokine family, *Mda-7* demonstrates antitumor effects across various cancers through multiple mechanisms, including apoptosis, proliferation, and angiogenesis[29]. Research has revealed the antitumor effect of *Mda-7* in neuroblastoma[30], breast cancer[31], colon cancer[32], and prostate cancer[33]. This evidence supports the notion that *Mda-7* could serve as an effective target to inhibit the development of GBM and increase treatment efficacy[24]. Our MTT results showed that the autophagy inhibitor CQ significantly enhanced the cytotoxic effect of *Mda-7*.

In this study, we confirmed through flow cytometry that the expression of LC3-II protein, as an autophagosomal marker, increased in U87 cells treated with Ad/*Mda-7* after CQ pharmacological intervention compared to the untreated control cells. The rise in

[DOI: 10.61882/ibj.5131]

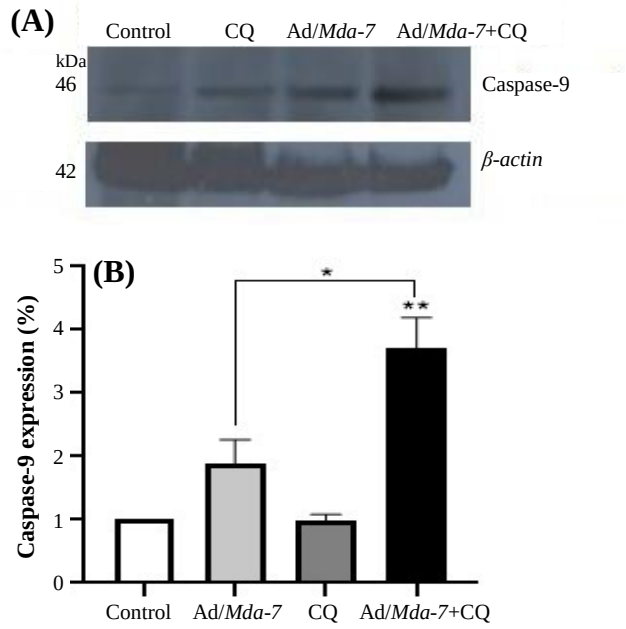

Fig. 7. **(**A) A representative Western blot of caspase-9 expression level after treatment with Ad/*Mda-7* and CQ in different groups in U87 cells. (B) The caspase-9 expression level was calculated by measuring its density using mage ImageJ software, which was standardized to the density of *β-actin*. Using ANOVA (one-way), a significant increase in the level of caspase-9 expression was observed in the combination treatment group compared to control group ($^{**}p < 0.003$) and Ad/ *Mda-7* monotherapy ($^{*}p < 0.01$).

LC3-II levels may be associated with blocking the final steps of autophagy and inhibiting autophagosomes-lysosome fusion. The increased LC3-II protein levels resulting from CQ treatment indicate an increase in autophagic flux or dysfunctional autophagy[34]. Unlike previous autophagy inhibitors, such as 3-methyladenine that suppress the initiation of autophagy, CQ blocks the late stage of autophagy. It works by interfering with the formation of autophagolysosomes, resulting in elevated LC3-II levels[26]. In addition, annexin V/PI staining and flow cytometry were performed to evaluate apoptotic U87 cells after monotherapy and combination therapy. The results obtained from the annexin assay showed that the combined treatment of *Mda-7*, a tumor suppressor gene, with CQ led to a significant increase in apoptosis in the GBM cell line. The activation of apoptosis depends on the involvement of at least two different pathways: an extrinsic pathway by caspase-8 activation and an intrinsic mitochondrial pathway by caspase-9 activation[35]. Since P38 is considered a tumor suppressor gene, its increased expression suppresses cell proliferation and apoptotic activity[36]. A promising strategy to induce apoptosis in glioma cells via the extrinsic pathway with potential amplification of the intrinsic pathway, is reactivating the TRAIL/TRAILR signaling pathway. This pathway induces the formation of death-inducing signaling complex and subsequently activates apoptosis initiator and effector caspases, with low toxicity at peripheral and cerebral levels[37]. TRAIL not only provides death signals through the extrinsic apoptotic pathway but also activates the intrinsic pathway through mitochondrial activation. Clinically, TRAIL induces the death in tumor while remaining essentially non-toxic to normal cells. After CQ treatment, TRAIL-induced apoptosis increases, resulting in G2/M phase arrest in pancreatic cancer cells[38].

In the present investigation, the increased levels of TRAIL (an extrinsic apoptosis factor) and elevated activity of key signaling proteins (caspase-9, P38 MAPK, and Bax) showed that the autophagy inhibitor CQ can significantly enhance the anticancer effect of Ad/*Mda-7*. This elevation occurs through the interaction

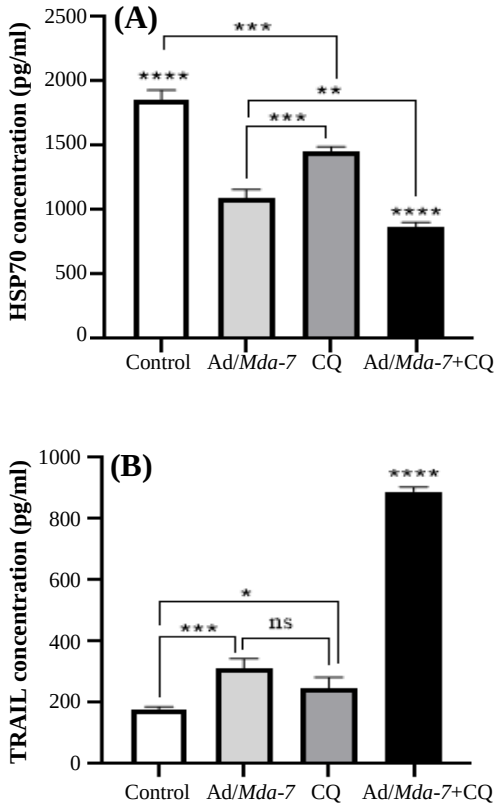

Fig. 8. Effect of co-treatment with Ad/Mda-7 on levels of HSP70 and TRAIL proteins. Quantify the levels of (A) HSP70 protein and (B) TRAIL protein after treatment with Ad/*Mda-7* and CQ as monotherapy or combination treatment groups after 48 h in U87 cells. Using ANOVA analysis (one-way), a significant decrease in the level of HSP70 protein produced ($^{**}p < 0.006$), ($^{***}p < 0.0001$), and ($^{****}p < 0.0001$) and conversely, a significant increase in the level of TRAIL protein produced ($^{*}P < 0.04$), ($^{***}p < 0.0001$), and ($^{****}p < 0.0001$) in the U87 cell line treated with all treatment groups compared to the control group.

[DOI: 10.61882/ibj.5131]

of the intrinsic and extrinsic pathways of apoptosis. In the combination therapy using Ad/*Mda-7* and CQ to inhibit autophagy, there was an accumulation of autophagosomes, leading to the increased ROS levels. ROS have been linked to class II programmed cell death, a cellular process characterized by autophagosome formation[39]. Under stress conditions, cancer cells can limit ROS accumulation by increasing cell-protective selective autophagy, including the inhibition of mitophagy to facilitate higher proliferation, metastasis, and resistance to drug therapy. Evidence suggests that the production of ROS via the intrinsic apoptotic pathway leads to cell death by damaging the mitochondrial membrane, releasing cytochrome C into the cytoplasm, and activating apoptosis through the ASK1/JNK (apoptotic regulatory kinase 1/C -Jun N-terminal kinase pathway)[40]. Therefore, the induction of ROS by CQ in combination with Ad/*Mda-7* significantly contributes to the antitumor function observed in U87 cells. This mechanism underscores the potential therapeutic efficacy of targeting ROS as a part of strategy for treating GBM, highlighting the importance of ROS modulation in anticancer therapies. Our results also showed that the synergistic effect of CQ with Ad/*Mda-7* can enhance the antitumor activity of Ad/*Mda-7* in U87 cells by reducing HSP70 protein expression levels.

RTKs are essential receptor proteins on the tumor cell membrane that trigger the activation of cancer signaling pathways. There is considerable evidence that HSP70 regulates a wide range of RTKs. Extracellular HSPBP1 and HSPA1A/B may synergistically activate the epidermal growth factor receptor[41]. Mechanistically, they enhance the phosphorylation and activation of the insulin-like growth factor I receptor to promote cell proliferation and migration. Furthermore, HSP70 influences the RAS pathway by modulating the KRAS protein and inhibiting downstream signaling components of RAF. Bag1 binds to and activates Raf1, which then activates the downstream extracellular ERKs[42].

Most research indicates that HSP70 has an activating role in regulating the RTKs-RAS-RAF-MEK-ERK signaling pathway. Besides, the PI3K/AKT/mTOR pathway is activated in various malignancies, resulting in tumor proliferation and therapeutic resistance. Typically, HSP70 promotes the PI3K/AKT/mTOR signaling pathway. Several pro-apoptotic proteins have been reported to be directly inhibited by HSP70. Medical research has found that high levels of the protein HSP70 in cancer cells are linked to a worse outcome for patients as cancer cells have more of this protein than healthy cells when the tumor grows[43].

Overexpression of HSP70 in tumor cells has a cytoprotective effect against proteotoxic stress and the resulting apoptosis. Inhibition of HSP70 can impair mitochondrial function, enhancing mitochondrial-mediated apoptosis. Moreover, HSP70 inhibition enhances AMPK-mediated phosphorylation of Beclin1, a key modulator of autophagy. Consistent with these findings, inhibition of HSP70 increases autophagy flux and works synergistically with autophagy inhibitors. Therefore, the inhibition of HSP70 could serve as a novel therapeutic strategy, potentially enhances treatment efficacy by simultaneously inhibiting autophagy[44].

In this study, we determined the expression levels of specific miRNAs as potential prognostic markers in malignant cells. Our results showed that the expression of *miR-7* and *miR-122* increased in treated U87 cells compared to control cells, indicating their involvement in antitumor activity. Notably, this treatment did not have a significant effect on miR-21 expression; in fact, its levels increased in the Ad/Mda-7-treated group. Furthermore, it showed an opposite effect, indicating that its antitumor effects were independent of this pathway. MiR-7 is one of the most potent tumor suppressors in various cancers and has been shown to regulate proliferation, migration, invasion, and metastasis[45]. Research has indicated that miR-7 downregulation in gastric cancer is associated with increased expression of LDH-A and chemoresistance[1]. Since the expression level of miR-7 significantly reduced in GBM, its overexpression can inhibit tumorigenesis and tumor progression[46]. In gliomas, energy metabolism associated with the Akt signaling pathway has been observed, particularly in aerobic glycolysis programs. However, the metabolic reactions regulating aerobic glycolysis and Akt activity are still obscure. One hypothesized mechanism is the control of IGF1R, a component of the upstream of AKT signaling pathway. Increased expression of miR-7 has been shown to suppress the glucose metabolic capacity and colony formation of glioma cells, an effect comparable to the "knockdown" of IGF-1R. This finding is consistent with data suggesting that miR-7 can bind to the 3' untranslated region of IGF-R, resulting in its downregulation[47]. Therefore, the upregulation of *miR-7* induced by CQ in combination with Ad/*Mda-7*, significantly enhanced its antitumor effect in U87 cells likely through tumor-suppressing properties and effectively targeting pathways involved in cancer development. Similarly, miR-122 is a tumor suppressor that is highly expressed in the liver; however, its expression is suppressed in hepatocellular carcinoma[48]. In breast cancer, miR-122 expression is also downregulated, and overexpression of miR-122 inhibits the proliferation and tumorigenesis of breast cancer cells

[DOI: 10.61882/ibj.5131]

by targeting the insulin-like growth factor-1 receptor[49]. Previous research have shown that miR-122 expression decreases in glioma cell lines. Moreover, plasma levels of miR-122 is a potential biomarker for glioma diagnosis and prognosis, and this miRNA plays an important role in mediating cell proliferation and apoptosis[50]. Therefore, the induction of *miR-122* by CQ in combination with Ad/*Mda-7* likely exerts antitumor effects in U87 cells by restoring the tumor-suppressive activity of *miR-122*, which in turn inhibits the key pathways involved in cancer cell proliferation and survival.

CONCLUSION

The combination treatment of CQ and Ad/*Mda-7* in U87 cells showed a positive antitumor effect through a strong mechanism. The accumulation of LC3-II protein, together with the generation of ROS, significantly increased apoptosis, as demonstrated by elevated levels of TRAIL and the activation of the proteins such as caspase-9, *P38 MAPK*, and *Bax*. The synergistic interaction between the extrinsic and intrinsic apoptotic pathways highlights the efficacy of CQ in combination with Ad/*Mda-7* in promoting apoptosis and inhibiting cancer cell viability. Furthermore, the combination therapy was associated with a decrease in HSP70 protein expression. This reduction is associated with positive antitumor responses, demonstrating the therapeutic potential of HSP70. Moreover, the increased expression of *miR-7* and *miR-122* induced by CQ and Ad/*Mda-7* significantly enhances the antitumor effects through their tumor suppressor properties. Taken together, these findings demonstrate the potential of CQ and Ad/*Mda-7* as a novel therapeutic strategy for treating GBM, highlighting the critical role of modulating autophagy, apoptotic cascades, and miRNAs for anticancer strategies.

DECLARATION

Acknowledgments

We would like to gratefully thank the researchers at Influenza and Respiratory Viruses Department, Pasteur Institute of Iran (Tehran), for their scientific support of this research project. No artificial intelligence services were used for the preparation of this manuscript.

Ethics approval

All experiments have been conducted in accordance with the guidelines of the Ethics Committee of National Institute for Medical Sciences Research Development, Tehran, Iran (ethical code: IR.NIMAD.REC.1396.321).

Consent to participate

Not applicable.

Consent for publication

All authors reviewed the results and approved the final version of the manuscript.

Authors' Contributions

SMB: writing–original draft preparation material, preparation, data collection, and analysis. AG: material preparation, data collection, and analysis. All authors contributed to the study conception and design.

Data availability

The datasets generated during the analysis in the current study are available from the corresponding author upon reasonable request.

Competing interests

The authors declare that they have no competing interests.

Funding

This work was supported by the National Institute for Medical Research Development (NIMAD), Iran (NIMAD [grant no. 962110] to Amir Ghaemi.

Supplementary information

The online version does contain supplementary material.

REFERNCES

1. Jin HF, Wang JF, Shao M, Zhou K, Ma X, Lv XP. Down-regulation of miR-7 in gastric cancer is associated with elevated LDH-A expression and chemoresistance to cisplatin. Front Cell Dev Biol. 2020:8:555937.
2. Tan Y, Sanders AJ, Zhang Y, Martin TA, Owen S, Ruge F, et al. Interleukin-24 (IL-24) expression and biological impact on HECV endothelial cells. Cancer Genomics Proteomics. 2015;12(5):243-50.
3. Persaud L, Mighty J, Zhong X, Francis A, Mendez M, Muharam H, et al. IL-24 promotes apoptosis through cAMP-dependent PKA pathways in human breast cancer cells. Int J Mol Sci. 2018;19(11):3561.
4. Fuchs Y, Steller H. Programmed cell death in animal development and disease. Cell. 2011;147(4):742-58.
5. Lefranc F, Kiss R. Autophagy, the trojan horse to combat glioblastomas. Neurosurg Focus. 2006;20(4):7.
6. Marino G, Niso-Santano M, Baehrecke EH, Kroemer G. Self-consumption: The interplay of autophagy and apoptosis. Nat Rev Mol Cell Biol. 2014;15(2):81-94.
7. Moloudi K, Neshasteriz A, Hosseini A, Eyvazzadeh N, Shomali M, Eynali S, et al. Synergistic effects of arsenic trioxide and tadiation: Triggering the intrinsic pathway of apoptosis. Iran Biomed J. 2017;21(5):330-7.

[DOI: 10.61882/ibj.5131]

8. Wu ST, Sun GH, Cha TL, Kao C-C, Chang -Y, Kuo S-C, et al. CSC-3436 switched tamoxifen-induced autophagy to apoptosis through the inhibition of AMPK/mTOR pathway. J Biomed Sci. 2016;23(1):60.
9. Amaravadi RK, Thompson CB. The roles of therapy-induced autophagy and necrosis in cancer treatment. Clin Cancer Res. 2007;13(24):7271-9.
10. Tasdemir E, Galluzzi L, Maiuri MC, Criollo A, Vitale I, Hangen E, et al. Methods for assessing autophagy and autophagic cell death. Methods Mol Biol. 2008:445:29–76.
11. Rabinowitz JD, White E. Autophagy and metabolism. Science. 2010;330(6009):1344-8.
12. White E. Deconvoluting the context-dependent role for autophagy in cancer. Nat Rev Cancer. 2012;12(6):401-10.
13. Zanotto-Filho A, Braganhol E, Klafke K, Figueiro F, Terra SR, Paludo FJ, et al. Autophagy inhibition improves the efficacy of curcumin/temozolomide combination therapy in glioblastomas. Cancer Lett. 2015;358(2):220-31.
14. Golden EB, Cho H-Y, Jahanian A, Hofman FM, Louie SG, Schonthal AH, et al. Chloroquine enhances temozolomide cytotoxicity in malignant gliomas by blocking autophagy. Neurosurg Focus. 2014;37(6):12.
15. Mei L, Chen Y, Wang Z, Wang J, Wan J, Yu C, et al. Synergistic anti-tumour effects of tetrandrine and chloroquine combination therapy in human cancer: A potential antagonistic role for p21. Br J Pharmacol. 2015;172(9):2232-45.
16. Lefort S, Joffre C, Kieffer Y, Givel A-M, Bourachot B, Zago G, et al. Inhibition of autophagy as a new means of improving chemotherapy efficiency in high-LC3B triple-negative breast cancers. Autophagy. 2014;10(12):2122-42.
17. Farrow JM, Yang JC, Evans CP. Autophagy as a modulator and target in prostate cancer. Nat Rev Urol. 2014;11(9):508-16.
18. Yang A, Kimmelman AC. Inhibition of autophagy attenuates pancreatic cancer growth independent of TP53/TRP53 status. Autophagy. 2014;10(9):1683-4.
19. Babazadeh SM, Zolfaghari MR, Zargar M, Baesi K, Hosseini SY, Ghaemi A. Interleukin-24-mediated antitumor effects against human glioblastoma via upregulation of P38 MAPK and endogenous TRAIL-induced apoptosis and LC3-II activation-dependent autophagy. BMC Cancer. 2023;23(1):519.
20. Amin W, Enam SA, Sufiyan S, Naeem S, Laghari AA, Bajwa MH, et al. Autophagy-associated markers LC3-II, ULK2 and microRNAs miR-21, miR-126 and miR-374 as a potential prognostic indicator for glioma patients. J Biol Life Sci. 2023:10:20944.
21. Yazdi AH, Zarrinpour V, Moslemi E, Forghanifard MM. A signature of three microRNAs is a potential diagnostic biomarker for glioblastoma. Iran Biomed J. 2022;26(4):301-12.
22. Liou G-Y, Storz P. Reactive oxygen species in cancer. Free Radical Res. 2010;44(5):479-96.
23. Park EJ, Min K-J, Choi KS, Kubatka P, Kruzliak P, Kim DE, et al. Chloroquine enhances TRAIL-mediated apoptosis through up-regulation of DR5 by stabilization of mRNA and protein in cancer cells. Sci Rep. 2016:6:22921.
24. Zhou N, Wei ZX, Qi ZX. Inhibition of autophagy triggers melatonin-induced apoptosis in glioblastoma cells. BMC Neurosci. 2019;20(1):63.
25. Kumar S, Yedjou CG, Tchounwou PB. Arsenic trioxide induces oxidative stress, DNA damage, and mitochondrial pathway of apoptosis in human leukemia (HL-60) cells. J Exp Clin Cancer Res. 2014;33(1):42.
26. Li J, Yang D, Wang W, Piao S, Zhou J, Saiyin W, et al. Inhibition of autophagy by 3-MA enhances IL-24-induced apoptosis in human oral squamous cell carcinoma cells. J Exp Clin Cancer Res. 2015;34(1):97.
27. Goncalves RM, Agnes JP, Delgobo M, de Souza PO, Thome MP, Heimfarth L, et al. Late autophagy inhibitor chloroquine improves efficacy of the histone deacetylase inhibitor SAHA and temozolomide in gliomas. Biochem Pharmacol. 2019:163:440-50.
28. Zhang J, Chen H, Chen C, Liu H, He Y, Zhao J, et al. Systemic administration of mesenchymal stem cells loaded with a novel oncolytic adenovirus carrying IL-24/endostatin enhances glioma therapy. Cancer Lett. 2021:509:26-38.
29. Rasoolian M, Kheirollahi M, Hosseini SY. MDA-7/interleukin 24 (IL-24) in tumor gene therapy: Application of tumor penetrating/homing peptides for improvement of the effects. Expert Opin Biol Ther. 2019;19(3):211-23.
30. Bhoopathi P, Lee N, Pradhan AK, Shen X-N, Das SK, Sarkar D, et al. mda-7/IL-24 induces cell death in neuroblastoma through a novel mechanism involving AIF and ATM. Cancer Res. 2016;76(12):3572-82.
31. Menezes ME, Shen X-N, Das SK, Emdad L, Guo C, Yuan F, et al. MDA-7/IL-24 functions as a tumor suppressor gene in vivo in transgenic mouse models of breast cancer. Oncotarget. 2015;6(35):36928-42.
32. Ma YF, Ren Y, Wu CJ, Zhao XH, Xu H, Wu DZ, et al. Interleukin (IL)-24 transforms the tumor microenvironment and induces anticancer immunity in a murine model of colon cancer. Mol Immunol. 2016:75:11-20.
33. Menezes ME, Bhoopathi P, Pradhan AK, Emdad L, Das SK, Guo C, et al. Role of MDA-7/IL-24 a multifunction protein in human diseases. Adv Cancer Res. 2018:138:143-82.
34. Cai Y, Cai J, Ma Q, Xu Y, Zou J, Xu L, et al. Chloroquine affects autophagy to achieve an anticancer effect in EC109 esophageal carcinoma cells in vitro. Oncol Lett. 2017;15(1):1143-8.
35. Chen HM, Lai ZQ, Liao HJ, Xie JH, Xian Y-F, Chen YL, et al. Synergistic antitumor effect of brusatol combined with cisplatin on colorectal cancer cells. Int J Mol Med. 2018;41(3):1447-54.
36. Soeda A, Lathia J, Williams BJ, Wu Q, Gallagher J, Androutsellis-Theotokis A, et al. The p38 signaling pathway mediates quiescence of glioma stem cells by regulating epidermal growth factor receptor trafficking. Oncotarget. 2017;8(20):33316-28.

[DOI: 10.61882/ibj.5131]

37. Mariani SM, Krammer PH. Differential regulation of TRAIL and CD95 ligand in transformed cells of the T and B lymphocyte lineage. Eur J Immunol. 1998;28(3):973-82.
38. Monma H, Iida Y, Moritani T, Okimoto T, Tanino R, Tajima Y, et al. Chloroquine augments TRAIL-induced apoptosis and induces G2/M phase arrest in human pancreatic cancer cells. Plos One. 2018:13(3):0193990.
39. Li S, Li Z, Chen S, Zhu Y, Li Y, Yin X, et al. Apoptotic and autophagic cell death induced in cervical cancer cells by a dual specific oncolytic adenovirus. Anticancer Drugs. 2023;34(3):361-72.
40. Samadi M, Mokhtari-Azad T, Nejati A, Norooz-Babaei Z, Foroushani AR, Haghshenas MR, et al. The antitumor effect of oncolytic respiratory syncytial virus via the tumor necrosis factor-alpha induction and ROS-bax-mediated mechanisms. BMC Cancer. 2023;23(1):803.
41. Evdonin A, Kinev A, Tsupkina N, Guerriero V, Raynes DA, Medvedeva N. Extracellular HspBP1 and Hsp72 synergistically activate epidermal growth factor receptor. Biol Cell. 2009;101(6):351-60.
42. Song J, Takeda M, Morimoto RI. Bag1–Hsp70 mediates a physiological stress signalling pathway that regulates Raf-1/ERK and cell growth. Nat Cell Biol. 2001;3(3):276-82.
43. Park YH, Seo JH, Park JH, Lee HS, Kim KW. Hsp70 acetylation prevents caspase-dependent/independent apoptosis and autophagic cell death in cancer cells. Int J Oncol. 2017;51(2):573-8.
44. Ferretti GD, Quaas CE, Bertolini I, Zuccotti A, Saatci O, Kashatus JA, et al. HSP70-mediated mitochondrial dynamics and autophagy represent a novel vulnerability in pancreatic cancer. Cell Death Differ. 2024;31(7):881-96.
45. Wuchty S, Arjona D, Li A, Kotliarov Y, Walling J, Ahn S, et al. Prediction of associations between microRNAs and gene expression in glioma biology. Plos One. 2011;6(2):14681.
46. Lages E, Guttin A, El Atifi M, Ramus C, Ipas H, Dupre I, et al. MicroRNA and target protein patterns reveal physiopathological features of glioma subtypes. Plos One. 2011;6(5):20600.
47. Morales-Martínez M, Vega MI. Role of microRNA-7 (MiR-7) in cancer physiopathology. Int J Mol Sci. 2022;23(16):9091.
48. Ahsani Z, Mohammadi-Yeganeh S, Kia V, Karimkhanloo H, Zarghami N, Paryan M. WNT1 gene from WNT signaling pathway is a direct target of miR-122 in hepatocellular carcinoma. Appl Biochem Biotechnol. 2017;181(3):884-97.
49. Wang B, Wang H, Yang Z. MiR-122 inhibits cell proliferation and tumorigenesis of breast cancer by targeting IGF1R. Plos One. 2012;7(10):47053.
50. Tang Y, Zhao S, Wang J, Li D, Ren Q, Tang Y. Plasma miR-122 as a potential diagnostic and prognostic indicator in human glioma. Neurol Sci. 2017;38(6):1087-92.

[DOI: 10.61882/ibj.5131]